Accurate Average Value Modeling of Synchronous Machine-Rectifier System Considering Stator Resistance

M. Shahnazari* and A. Vahedi*

Abstract: An accurate average value model of synchronous machine-rectifier system considering the effect of stator resistance is derived in this paper. A proper voltage-behind-reactance synchronous machine model without any approximations is used for the generator that allows effective calculation of commutation displacement angle. All rectification modes of the rectifier are studied. A detailed switching model is implemented and validated against experimental measurements. The described average value model is evaluated through comparison of detailed simulation results and average model in time domain.

Keywords: Synchronous Machine, Rectifier, Average-Value Model, Commutation Angle.

1 Introduction

Synchronous generator-rectifier systems are widely used in brushless excitation of synchronous generators, wind power generators, aircraft electrical systems, automotives, etc. The detailed models of these systems, in which the switching of each diode is represented, can be readily established using various simulation software packages. Using switching models to study the machine-rectifier system, makes it unsuitable for linearization and control purpose applications. Also, because of the need to keep the maximum simulation time step well below the switching period, these simulations are time and memory consuming. Therefore, average models have been used to investigate these systems.

There are two main ways to derive average models for diode rectifiers, namely transfer function method ([1]-[5]) and mathematical derivation method ([6]-[10]). The transfer function method founds the relationship between the input and output of the rectifier using a black box approach. This method is very simple to implement, avoids the complex calculation of differential equations, and takes into account the nonlinearity effects, but it is time-consuming, not convenient for variable frequency systems and difficult to include and improve for model dynamics. In contrast, the mathematical derivation method is not subject to these limitations, as closed-form expressions are used to determine the average input and output voltages and currents.

An average value machine-rectifier model that allows linking of dq-axis machine model to dc quantities was derived in [7]. A reduced-order machine model with neglected stator dynamics and fast transients associated with the rotor windings was used in [10] in order to model the brushless excitation system.

In [11] a general simulation method for the investigation of commutation phenomena and faults in a synchronous machine-rectifier system is presented and the influence of stator leakage inductance, q-axis damper winding inductance and the load resistance on the commutation phenomena has been studied. The average value models for twelve-pulse transformer-diode rectifier units used in more-electric aircraft power systems have been developed in [12] and [13].

In this paper, an efficient voltage-behind-reactance (VBR) synchronous machine model without any approximations is used for the generator. The displacement angle of commutation is effectively calculated based on VBR model equations. All modes of rectifier operation are considered in average value modeling.

2 Machine Model

In a generator-rectifier system, pairs of stator terminals of the generator are short circuited six times per one cycle. Therefore its characteristics are different from ordinary synchronous machines and a suitable full-order model is needed for accurate modeling of machine-converter system behavior.

In [7] a dynamic approximate VBR model has been used in the analysis and simulation of synchronous machine-converter system, under the assumption that

Iranian Journal of Electrical & Electronic Engineering, 2009.
Paper first received 6 Dec. 2009 and in revised form 10 Nov. 2009.
* The Authors are with the Center of Excellence for Power System Automation and Operation, Iran University of Science & Technology, Tehran, Iran.
E-mails: shahnazari@iust.ac.ir, avahedi@iust.ac.ir

the rotor flux linkages don't change over short time intervals. In VBR model used in this study, the derivatives of the rotor flux linkages are algebraically incorporated into the stator voltage equations. The stator circuit is expressed in phase coordinates using the physical currents as the independent variables while the rotor subsystem is expressed in dq rotor reference frame, with the flux linkages used as the independent variables. A detailed derivation of the exact VBR model can be found in [14]. In this formulation, the stator voltage equation can be expressed as:

$$V_{abcs} = R_{abcs}(\theta_r).i_{abcs} + p[L''_{abcs}(\theta_r).i_{abcs}] + E''_{abcs} \quad (1)$$

The resistance (R_{abcs}) and inductance (L''_{abcs}) matrices are expressed by

$$R_{abcs}(\theta_r) = \mathrm{diag}[rs, rs, rs] \quad (2)$$

$$L''_{abcs}(\theta_r) = \begin{bmatrix} L_S(2\theta_r) & L_M(2\theta_r - \frac{2\pi}{3}) & L_M(2\theta_r + \frac{2\pi}{3}) \\ L_M(2\theta_r - \frac{2\pi}{3}) & L_S(2\theta_r - \frac{4\pi}{3}) & L_M(2\theta_r) \\ L_M(2\theta_r + \frac{2\pi}{3}) & L_M(2\theta_r) & L_S(2\theta_r + \frac{4\pi}{3}) \end{bmatrix} \quad (3)$$

where

$$L_S(.) = L_{ls} + L_a - L_b\cos(.) \quad (4)$$

$$L_M(.) = -\frac{L_a}{2} - L_b\cos(.) \quad (5)$$

$$L_a = \frac{L''_{md} + L''_{mq}}{3} \quad (6)$$

$$L_b = \frac{L''_{md} - L''_{mq}}{3} \quad (7)$$

The magnetizing inductances L''_{md} and L''_{mq} are calculated as:

$$L''_{md} = \left(\frac{1}{L_{md}} + \frac{1}{L_{lf}} + \frac{1}{L_{lkd}}\right)^{-1} \quad (8)$$

$$L''_{mq} = \left(\frac{1}{L_{mq}} + \frac{1}{L_{lkq1}} + \frac{1}{L_{lkq2}}\right)^{-1} \quad (9)$$

The voltages E''_{abcs} are defined as:

$$E''_{abcs} = [K(\theta_r)]^{-1}\begin{bmatrix} e''_q & e''_d & 0 \end{bmatrix}^T \quad (10)$$

$$e''_q = \omega_r \lambda''_d + (\frac{L''_{mq}}{L^2_{lkq1}} r_{kq1}(\lambda''_q - \lambda_{kq1}) + \frac{L''_{mq}}{L^2_{lkq2}} r_{kq2}(\lambda''_q - \lambda_{kq2})) + ((\frac{L''_{mq}}{L_{lkq1}})^2.r_{kq1} + (\frac{L''_{mq}}{L_{lkq2}})^2.r_{kq2}).iq \quad (11)$$

$$e''_d = -\omega_r \lambda''_q + \frac{L''_{md}}{L_{lf}} v_f + \frac{L''_{md}}{L^2_{lf}} r_f(\lambda''_d - \lambda_f) + \frac{L''_{md}}{L^2_{lkd}} r_{kd}(\lambda''_d - \lambda_{kd}) + ((\frac{L''_{md}}{L_{lf}})^2.r_f + (\frac{L''_{md}}{L_{lkd}})^2.r_{kd}).id \quad (12)$$

$$\lambda''_q = L''_{mq}.(\frac{\lambda_{kq1}}{L_{lkq1}} + \frac{\lambda_{kq2}}{L_{lkq2}}) \quad (13)$$

$$\lambda''_d = L''_{md}(\frac{\lambda_f}{L_{lf}} + \frac{\lambda_{kd}}{L_{lkd}}) \quad (14)$$

Rotor dynamics are represented by the following equations:

$$p\lambda_{kqi} = -\frac{r_{kqi}}{L_{lkqi}}(\lambda_{kqi} - \lambda_{mq}) \qquad i = 1,2 \quad (15)$$

$$p\lambda_f = -\frac{r_f}{L_{lf}}(\lambda_f - \lambda_{md}) \quad (16)$$

$$p\lambda_{kd} = -\frac{r_{kd}}{L_{lkd}}(\lambda_{kd} - \lambda_{md}) \quad (17)$$

$$\lambda_{mq} = L''_{mq}(\frac{\lambda_{kq1}}{L_{lkq1}} + \frac{\lambda_{kq2}}{L_{lkq2}} + i_q) \quad (18)$$

$$\lambda_{md} = L''_{md}(\frac{\lambda_f}{L_{lf}} + \frac{\lambda_{kd}}{L_{llkd}} + i_d) \quad (19)$$

As can be seen in Eqs. (11) and (12), contrary to reduced order machine model, considering the derivatives of the rotor flux linkages on the stator dynamics provide an added effective stator resistance (third term) and an induced back emf (second term) on each of the stator windings. The induced voltage is independent of the rotor speed. Hence, forming the reduced order model is equivalent to neglecting the added stator resistance and the induced voltage due to the changing rotor flux linkages which in some cases yields an unstable representation of the synchronous machine.

3 Rectifier Average Value Modeling

For a three phase machine-rectifier system supplying an inductive load (Fig. 1), the rectification process can be divided into three distinct modes 1-3, which occur in numerical sequence as load current (rectifier's output current) increases from zero. The rectifier average value model computes the average currents flowing in the generator terminals from the load current and generator parameters. Here, we suppose that the output inductance (L_l) is large enough that the load current varies slowly.

Because of symmetry, it is sufficient to consider a $\pi/3$ interval for example when D2 starts conducting at phase angle $\theta_r=\alpha$ and ends at $\theta_r=\alpha+\pi/3$ where θ_r defines

as the voltage angle of phase (a) and α is delay angle. As a consequence of generator and load inductances, transfer of current from a diode to another (commutation) in rectifier, creates temporary phase to phase short circuit during the cycle.

3.1 Discontinuous Mode

At relatively low values of load current, the commutation of current is fast and ends before the next one begins (discontinuous commutation). At the start of considered interval, the load current begins to transfer from phase b to phase c, hence, D1, D2 and D6 are in conduction (commutation period). Both the bridge current and diodes currents are discontinuous in this mode. Commutation period starts at $\theta_r = \delta$ and lasts for u where u is the commutation angle ($0 \le u < \pi/3$). D1, D2 and D6 are in conduction in this period until D6 turns off at $\theta_r = \delta + u$ and conduction period is started wherein D1 and D2 conduct during ($u+\delta \le \theta_r < \delta + \pi/3$).

Using the exact VBR model mentioned above for the synchronous generator, displacement angle δ may be calculated using the back emf voltages given by Eq. (11) and Eq. (12):

$$\delta = \tan^{-1}(e_d^{"} / e_q^{"}) \tag{20}$$

The abc currents of stator are:

$$i_{abc}(\theta_r) = \begin{cases} \begin{bmatrix} -i_{dc} & i_{dc} - i_2 & i_2 \end{bmatrix}^T & \text{for } \delta \le \theta_r < \delta + u \\ \begin{bmatrix} -i_{dc} & 0 & i_{dc} \end{bmatrix}^T & \text{for } \delta + u \le \theta_r < \delta + \frac{\pi}{3} \end{cases} \tag{21}$$

where i_{dc} is the rectifier output current and i_2 is the current of D2 increases from $i_2(\delta)=0$ to $i_2(\delta+u)=i_{dc}$. The average rectifier output voltage may be expressed as:

$$\overline{v_{dc}} = \frac{3}{\pi} \int_{\delta}^{\delta+\frac{\pi}{3}} (v_{ar} - v_{cr}) d\theta_r \tag{22}$$

which may be extracted as

$$\overline{v_{dc}} \approx \frac{3}{\pi} \int_{\delta}^{\delta+\frac{\pi}{3}} (\frac{d}{dt}\lambda_{ar} - \frac{d}{dt}\lambda_{cr}) d\theta_r - 2 r_s i_{dc} = \frac{3}{\pi}\omega_r [(\lambda_{ar} - \lambda_{cr})_{\theta_r = \delta + \frac{\pi}{3}} - (\lambda_{ar} - \lambda_{cr})_{\theta_r = \delta}] - 2 r_s i_{dc} \tag{23}$$

where

$$\begin{bmatrix} \lambda_{ar} \\ \lambda_{br} \\ \lambda_{cr} \end{bmatrix} = K^{-1}(\theta_r).\lambda_{qd0} = \begin{bmatrix} \lambda_q.\cos(\theta_r) + \lambda_d.\sin(\theta_r) \\ \lambda_q.\cos(\theta_r - \frac{2\pi}{3}) + \lambda_d.\sin(\theta_r - \frac{2\pi}{3}) \\ \lambda_q.\cos(\theta_r + \frac{2\pi}{3}) + \lambda_d.\sin(\theta_r + \frac{2\pi}{3}) \end{bmatrix} \tag{24}$$

$$\lambda_{ar} - \lambda_{cr} = \sqrt{3} \begin{bmatrix} (L_q^{"}.i_q + \lambda_q^{"}).\sin(\theta_r + \frac{\pi}{3}) \\ -(L_d^{"}.i_d + \lambda_d^{"}).\cos(\theta_r + \frac{\pi}{3}) \end{bmatrix} \tag{25}$$

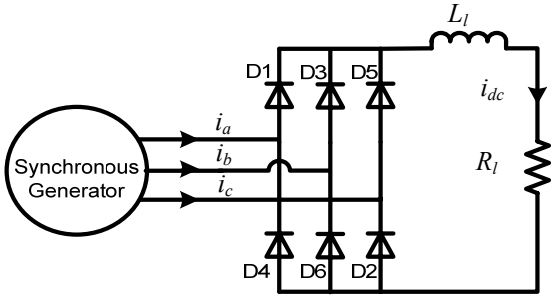

Fig. 1 Synchronous generator-rectifier system

The currents i_q and i_d may be computed at $\theta_r = \delta$ and $\theta_r = \delta + \pi/3$ using Eq. (21). Then:

$$i_{qd}(\theta_r) = \frac{2\sqrt{3}}{3} i_{dc} \begin{bmatrix} \sin(\delta - \frac{\pi}{3}) & -\cos(\delta - \frac{\pi}{3}) \end{bmatrix}^T \quad \text{for} \quad \theta_r = \delta, \ \delta + \frac{\pi}{3} \tag{26}$$

$$\begin{aligned} &(\lambda_{ar} - \lambda_{cr})_{\theta_r = \delta + \frac{\pi}{3}} - (\lambda_{ar} - \lambda_{cr})_{\theta_r = \delta} = \\ &-2.L_d^{"}.\sin(\delta + \pi/6).\cos(\delta) i_{dc} + \\ &2.L_q^{"}.\cos(\delta + \pi/6).\sin(\delta) i_{dc} \\ &+ \sqrt{3}.\lambda_d^{"}.\cos(\delta) - \sqrt{3}.\lambda_q^{"}.\sin(\delta) \end{aligned} \tag{27}$$

The average dc voltage is

$$\begin{aligned} \overline{v_{dc}} = &\frac{3}{\pi}\omega_r(-2.L_d^{"}.\sin(\delta + \pi/6).\cos(\delta) i_{dc} + \\ &2.L_q^{"}.\cos(\delta + \pi/6).\sin(\delta) i_{dc} + \sqrt{3}.\lambda_d^{"}.\cos(\delta) \\ &-\sqrt{3}.\lambda_q^{"}.\sin(\delta)) - 2 r_s i_{dc} \end{aligned} \tag{28}$$

During commutation period, D2 and D6 conduct simultaneously and if the diode resistance is neglected, a short-circuit between phases b and c is in effect (v_{br}-v_{cr}=0). Then:

$$\lambda_{br} - \lambda_{cr} = C \tag{29}$$

where C is a constant. Using Eq. (24):

$$\begin{aligned} &\lambda_{br} - \lambda_{cr} = \\ &\sqrt{3}\left[(L_q^{"}.i_q + \lambda_q^{"}).\sin\theta - (L_d^{"}.i_d + \lambda_d^{"}).\cos\theta\right] \end{aligned} \tag{30}$$

Transforming Eq. (21) to qd-axes and substituting into Eq. (30) yields:

$$\begin{aligned} &\lambda_{br} - \lambda_{cr} = -2.i_2(L_q^{"}.\sin^2\theta + L_d^{"}.\cos^2\theta) + \\ &2.i_{dc}.[L_q^{"}.\sin\theta.\sin(\theta - \frac{\pi}{3}) + L_d^{"}.\cos\theta.\cos(\theta - \frac{\pi}{3})] + \\ &\sqrt{3}.\lambda_q^{"}.\sin\theta - \sqrt{3}.\lambda_d^{"}.\cos\theta = C \end{aligned} \tag{31}$$

Evaluating this expression at $\theta_r = \delta$ and $\theta_r = \delta + u$, we obtain:

$$C = 2[L_q^{"}.\sin\delta.\sin(\delta-\frac{\pi}{3}) + L_d^{"}.\cos\delta.\cos(\delta-\frac{\pi}{3})].i_{dc} + \sqrt{3}.\lambda_q^{"}.\sin\delta - \sqrt{3}.\lambda_d^{"}.\cos\delta \quad (32)$$

and

$$[-(L_d^{"}+L_q^{"}) + 2(L_d^{"}-L_q^{"}).\cos(2\delta+u).\sin(u-\frac{\pi}{6})]i_{dc} = \sqrt{3}.\lambda_d^{"}.(\cos(\delta+u)-\cos(u)) - \sqrt{3}.\lambda_q^{"}.(\sin(\delta+u)-\sin(\delta)) \quad (33)$$

Equation (33) may be solved numerically for the commutation angle u. Calculation of u and C allows the computation of the average qd-axis rotor currents. Eq. (31) is solved for i_2 and substituted into Eq. (21), which is transformed to dq rotor reference frame. The currents of the commutation period are thus:

$$i_{qd1}(\theta_r) = \frac{2\sqrt{3}}{3}\begin{bmatrix} i_{dc}.\sin(\theta_r-\frac{\pi}{3}) - i_2.\sin(\theta_r) \\ -i_{dc}.\cos(\theta_r-\frac{\pi}{3}) + i_2.\cos(\theta_r) \end{bmatrix} \quad (34)$$

and their average value is $\bar{i}_{qd1} = \frac{3}{\pi}\int_{\delta}^{\delta+u} i_{qd1}(\theta_r).d\theta_r$ which is evaluated numerically.

On the other hand, the currents of the conduction period and their average value (which may be computed analytically) are:

$$i_{qd2}(\theta_r) = \frac{2\sqrt{3}}{3} i_{dc}\begin{bmatrix} -\sin(\theta_r+\frac{\pi}{3}) \\ \cos(\theta_r+\frac{\pi}{3}) \end{bmatrix} \quad (35)$$

$$\bar{i}_{qd2} = \frac{2\sqrt{3}}{\pi} i_{dc}\begin{bmatrix} \cos(\delta+\frac{2\pi}{3}) - \cos(\delta+u+\frac{\pi}{3}) \\ \sin(\delta+\frac{2\pi}{3}) - \sin(\delta+u+\frac{\pi}{3}) \end{bmatrix} \quad (36)$$

The total qd-axes currents average value during this mode is $\bar{i}_{qd} = \bar{i}_{qd1} + \bar{i}_{qd2}$.

Discontinuous mode ends when the commutation angle u reaches $\pi/3$ as i_{dc} increases. Then, each commutation period occurs simultaneously after previous one.

3.2 Continuous Mode

If load current increases more than its value at the end of discontinuous mode, current transfer between D5 and D1 is not finished at $\theta_r=\delta$ and commutation of current between D6 and D2 cannot begin. The commutation period, then, is delayed in starting.

In this mode commutation becomes continuous and three diodes are always conducting. The commutation angle u remains constant at $\pi/3$ but start of commutation is delayed by an angle α which varies from 0 to $\pi/6$ as i_{dc} increases. This delay is added to the displacement angle δ which is calculated using Eq. (20) and α is obtained solving a nonlinear equation extracted subsequently.

The stator currents are:

$$i_{abc}(\theta_r) = \begin{bmatrix} -i_{dc} & i_{dc}-i_2 & i_2 \end{bmatrix}^T \quad \text{for } \delta+\alpha \le \theta_r < \delta+\alpha+\frac{\pi}{3} \quad (37)$$

The current i_2 increases from $i_2(\delta+\alpha)=0$ to $i_2(\delta+\alpha+\pi/3)=i_{dc}$. During this interval:

$$i_{qd}(\theta_r) = \frac{2\sqrt{3}}{3}.i_{dc}\begin{bmatrix} \sin(\delta+\alpha-\frac{\pi}{3}) \\ -\cos(\delta+\alpha-\frac{\pi}{3}) \end{bmatrix} \quad \text{for } \theta_r = \delta+\alpha,\ \delta+\alpha+\frac{\pi}{3} \quad (38)$$

Substituting these currents into Eq. (25) and Eq. (23), yields us

$$\overline{v_{dc}} = \frac{3}{\pi}\omega_r\left(\sqrt{3}.\lambda_d^{"}.\cos(\delta+\alpha) - \sqrt{3}.\lambda_q^{"}.\sin(\delta+\alpha) - \left[\frac{1}{2}(L_d^{"}+L_q^{"}) + (L_d^{"}-L_q^{"}).\cos(2\delta+2\alpha-\frac{\pi}{3})\right].i_{dc}\right) - 2r_s i_{dc} \quad (39)$$

Substituting Eq. (37) into Eq. (31), evaluating it at $\theta_r=\delta+\alpha$ and $\theta_r=\delta+\alpha+\pi/3$ and equating the two results yields:

$$[(L_d^{"}+L_q^{"}) + (L_d^{"}-L_q^{"}).\sin(2\delta+2\alpha-\frac{\pi}{6})].i_{dc} = \sqrt{3}.\lambda_d^{"}.\sin(\delta+\alpha+\frac{\pi}{6}) + \sqrt{3}.\lambda_q^{"}.\cos(\delta+\alpha+\frac{\pi}{6}) \quad (40)$$

This equation is solved numerically for α. The qd-axes rotor reference currents during this mode is the same as commutation period in discontinuous mode and their average is:

$$\bar{i}_{qd} = \frac{3}{\pi}\int_{\delta+\alpha}^{\delta+\alpha+\frac{\pi}{3}} i_{qd}(\theta_r).d\theta_r \quad (41)$$

which is evaluated numerically.

Continuous commutation mode ends when the delay angle α equals $\pi/6$ as load current increases.

3.3 Simultaneous Commutation Mode

By the increase of load current, commutation between D5 and D1 is not completed at the end of continuous commutation mode ($\theta=\delta+\pi/6$) and current will begin to transfer between D6 and D2. Thus, for a period all three phases are carrying current.

In this mode the delay angle α remains fixed at $\pi/6$ and the commutation angle u increases from $\pi/3$ to $2\pi/3$ as i_{dc} increases. The delay angle is $\delta+\pi/6$ which δ is calculated using Eq. (20).

At start of this mode ($\theta_r=\delta+\pi/6$), two commutations are taking place simultaneously, four diodes are conducting (1, 5, 6 and 2), and a three phase short-circuit occurs, so $v_{dc}=0$. The commutation of D1 is at a further stage than D2, thus $i_1(\delta+\pi/6)=i_m$ and $i_2(\delta+\pi/6)=0$. At $\theta_r=\delta+u-\pi/6$, commutation of D5 and D1 finishes and three diodes conducting (1, 2 and 6), applying a line-to-line short-circuit to the generator terminals ($i_1(\delta+u-\pi/6)=i_{dc}$, $i_2(\delta+u-\pi/6)=i_n$). This interval ends at $\theta=\delta+\pi/2$ when D3 starts conducting and $i_2(\delta+\pi/2)=i_m$ due to symmetry.

The abc currents in this mode are:

$$i_{abc}(\theta_r)=\begin{cases}\begin{bmatrix}-i_1 & i_{dc}-i_2 & -i_{dc}+i_1+i_2\end{bmatrix}^T \\ \qquad \text{for } \delta+\frac{\pi}{6}\le\theta_r<\delta+u-\frac{\pi}{6} \\ \begin{bmatrix}-i_{dc} & i_{dc}-i_2 & i_2\end{bmatrix}^T \\ \qquad \text{for } \delta+u-\frac{\pi}{6}\le\theta_r<\delta+\frac{\pi}{2}\end{cases} \quad (42)$$

During the first interval (four diode conducting), v_{ar}-$v_{cr}=0$ and v_{br}-$v_{cr}=0$ then:

$$\lambda_{br}-\lambda_{cr}=C_1 \quad (43)$$

$$\lambda_{ar}-\lambda_{cr}=C_2 \quad (44)$$

Equation (43) is valid for the second interval (three diodes conducting) too.

Transforming the abc currents into qd-reference frame and substituting them into Eq. (30) results:

$$\lambda_{br}-\lambda_{cr}=2.(i_{dc}-i_2)(L''_q.\sin^2\theta_r+L''_d.\cos^2\theta_r)- 2i_1[L''_q\sin\theta_r.\sin(\theta_r+\frac{\pi}{3})+L''_d\cos\theta_r.\cos(\theta_r+\frac{\pi}{3})] +\sqrt{3}\lambda''_q.\sin\theta_r-\sqrt{3}\lambda''_d.\cos\theta_r=C_1 \quad (45)$$

Substitution of the values of i_1 and i_2 at $\theta_r=\delta+\pi/6$ and $\theta_r=\delta+\pi/2$ into Eq. (45) yields:

$$2.i_m.(L''_q.\cos(\delta).\sin(\delta+\frac{\pi}{6})-L''_d.\sin(\delta).\cos(\delta+\frac{\pi}{6})) +C_1=2.i_{dc}.(L''_q.\sin^2(\delta+\frac{\pi}{6})-L''_d.\cos^2(\delta+\frac{\pi}{6}))+ \sqrt{3}.\lambda''_q.\sin(\delta+\frac{\pi}{6})-\sqrt{3}.\lambda''_d.\cos(\delta+\frac{\pi}{6}) \quad (46)$$

$$2.i_m.(L''_q.\cos^2(\delta)+L''_d.\sin^2(\delta))+C_1= 2.i_{dc}.(L''_q.\cos(\delta).\sin(\delta+\frac{\pi}{6})-L''_d.\sin(\delta).\cos(\delta+\frac{\pi}{6})) \sqrt{3}.\lambda''_q.\cos(\delta)+\sqrt{3}.\lambda''_d.\sin(\delta) \quad (47)$$

Solving Eq. (46) and Eq. (47) for i_m and C_1 results:

$$i_m=\frac{\sqrt{3}.\lambda''_q.\sin(\delta-\frac{\pi}{6})-\sqrt{3}.\lambda''_d.\cos(\delta-\frac{\pi}{6})}{-\frac{1}{2}(L''_d+L''_q)+(L''_q-L''_d).\sin(2\delta-\frac{\pi}{6})}+ \frac{\frac{1}{2}(L''_d+L''_q)+(L''_d-L''_q).\cos(2\delta)}{-\frac{1}{2}(L''_d+L''_q)+(L''_q-L''_d).\sin(2\delta-\frac{\pi}{6})}.i_{dc} \quad (48)$$

$$C_1=((L''_d+L''_q)+(L''_d-L''_q).\cos(2\delta+\frac{\pi}{3})).i_{dc}+ (-\frac{1}{2}(L''_d+L''_q)+(L''_d-L''_q).\sin(2\delta+\frac{\pi}{6})).i_m+ \sqrt{3}.\lambda''_q.\sin(\delta+\frac{\pi}{6})-\sqrt{3}.\lambda''_d.\cos(\delta+\frac{\pi}{6}) \quad (49)$$

Also, i_n may be calculated by evaluating Eq. (45) at $\theta_r=\delta+u-\pi/6$:

$$i_n=\frac{\sqrt{3}.\lambda''_q.\sin(\delta+u-\frac{\pi}{6})-\sqrt{3}.\lambda''_d.\cos(\delta+u-\frac{\pi}{6})}{(L''_d+L''_q)+(L''_d-L''_q).\cos(2\delta+2u-\frac{\pi}{3})}+ \frac{\left[\frac{1}{2}(L''_d+L''_q)+(L''_d-L''_q).\sin(2\delta+2u-\frac{\pi}{6})\right].i_{dc}-C_1}{(L''_d+L''_q)+(L''_d-L''_q).\cos(2\delta+2u-\frac{\pi}{3})} \quad (50)$$

Equation (44) is valid only for the first interval that four diodes conducting. Inserting dq currents at interval $\delta+\pi/6\le\theta_r<\delta+u-\pi/6$ into Eq. (25) and evaluating the resultant equation at $\theta_r=\delta+\pi/6$ and $\theta_r=\delta+u-\pi/6$ results:

$$C_2=(\frac{1}{2}(L''_d+L''_q)+(L''_q-L''_d).\sin(2\delta+\frac{\pi}{6})).i_{dc}- ((L''_d+L''_q)+(L''_q-L''_d).\cos(2\delta)).i_m+ \sqrt{3}.\lambda''_q.\cos(\delta)+\sqrt{3}.\lambda''_d.\sin(\delta) \quad (51)$$

$$\left[-\frac{1}{2}(L''_q+L''_d)+(L''_d-L''_q).\sin(2\delta+2u+\frac{\pi}{6})\right].i_{dc}- \left[\frac{1}{2}(L''_q+L''_d)+(L''_d-L''_q).\cos(2\delta+2u)\right].i_n -\sqrt{3}.\lambda''_d.\cos(\delta+u+\frac{\pi}{6}) +\sqrt{3}.\lambda''_q.\sin(\delta+u+\frac{\pi}{6})-C_2=0 \quad (52)$$

The nonlinear Eq. (53) is solved numerically for u. During the first interval ($\delta+\pi/6\le\theta_r<\delta+u-\pi/6$), $v_{dc}=0$. So, it is sufficient to calculate v_{dc} for second interval ($\delta+u-\pi/6\le\theta_r<\delta+\pi/2$). Using Eq. (48) - Eq. (50) in conjunction with Eq. (23):

$$\overline{v_{dc}} = \frac{3}{\pi}\omega_r(\sqrt{3}.\lambda_d^{"}.\cos(\delta+\frac{\pi}{6}) - \sqrt{3}.\lambda_q^{"}.\sin(\delta+\frac{\pi}{6}) - ((L_d^{"}+L_q^{"}) + (L_q^{"}-L_d^{"}).\sin(2\delta-\frac{\pi}{6}))i_{dc} + (\frac{1}{2}(L_d^{"}+L_q^{"}) + (L_q^{"}-L_d^{"}).\sin(2\delta+\frac{\pi}{6}))i_m) - 2r_s i_{dc} \quad (53)$$

To compute dq-axes current during first interval, it is essential to obtain $i_1(\theta_r)$ and $i_2(\theta_r)$:

$$i_1(\theta_r) = -\frac{C_1}{3L_d^{"}.L_q^{"}}\left[\frac{1}{2}(L_d^{"}+L_q^{"}) + (L_d^{"}-L_q^{"}).\sin(2\theta_r+\frac{\pi}{6})\right] + \frac{\lambda_d^{"}}{L_d^{"}}.\sin\theta_r + \frac{\lambda_q^{"}}{L_q^{"}}.\cos\theta_r \quad (54)$$

$$i_2(\theta_r) = i_{dc} + \frac{C_1}{3L_d^{"}.L_q^{"}}\left[\frac{1}{2}(L_d^{"}+L_q^{"}) - (L_d^{"}-L_q^{"}).\cos(2\theta_r)\right] + \frac{\lambda_d^{"}}{L_d^{"}}.\sin(\theta_r+\frac{\pi}{3}) + \frac{\lambda_q^{"}}{L_q^{"}}.\cos(\theta_r+\frac{\pi}{3}) \quad (55)$$

Thus the average qd-axes currents may be calculated during two intervals using analytical and numerical integration.

4 Computer Studies and Experimental Results

A detailed switching model of a converter connected synchronous generator has been implemented in Matlab Sim-Power System Toolbox. To validate this model, the detailed simulation is compared with online measurements taken on a laboratory synchronous generator. The measured machine is a small 1.2 kVA, 220 V, 1500 rpm synchronous generator which its parameters are listed in Table 1. The system starts up with initial conditions corresponding to steady state operation with constant field voltage at 97.7 V and nominal generator speed. The initial load resistance is 72.2 Ω which is changed to 33.2 Ω at t=0.1 sec. The time-domain comparison between the detailed switching model and the corresponding experimental responses are presented in Fig. 2 and Fig. 3, wherein it is shown that the detailed model portrays the response of the actual hardware system. The proposed machine-converter average value model has also been implemented in Matlab in order to fully compare its operation against detailed simulation. The machine under study is a 3.7 kW, 230 V, 1800 rpm synchronous generator [7]. In order to study the operation of the rectifier in discontinuous mode, a load resistance of 40 Ω is considered at first so that at time t=0.3 sec., decreases to 20 Ω. The load current and a-phase voltage are plotted in Fig. 4 and Fig. 5. The computer generated response of the detailed model and average value model are depicted in Figs. 6-8.

Table 1 Synchronous generator parameters

r_s=1.68 Ω	L_{ls}=6.5 mH	L_{md}=110.1 mH	L_{mq}=95.5 mH
r_f=1.72 Ω	L_{lf}=24.3 mH	r_{kd}=15.41 Ω	L_{kd}=6.4 mH
r_{kq1}=60.3Ω	L_{kq1}=10.21 mH	r_{kq2}=50.6Ω	L_{kq2}=33 mH

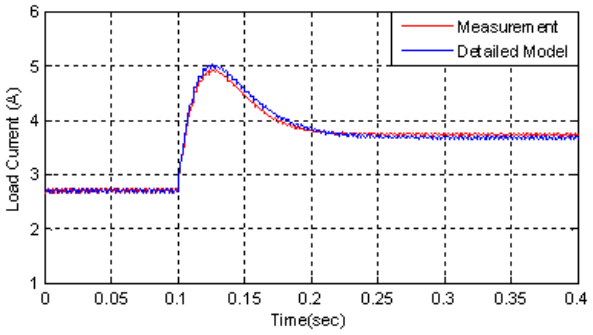

Fig. 2 Load current at resistance step from 72.2 Ω to 33.2 Ω

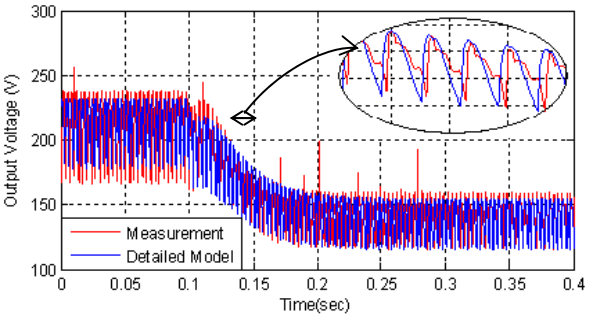

Fig. 3 Output voltage at resistance step from 72.2Ω to 33.2 Ω

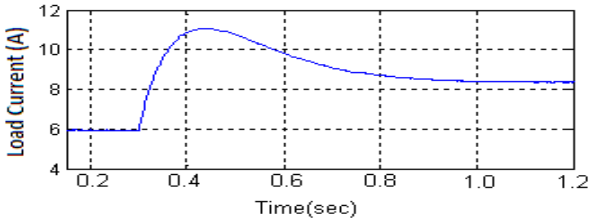

Fig. 4 Load current at resistance step from 40 Ω to 20 Ω

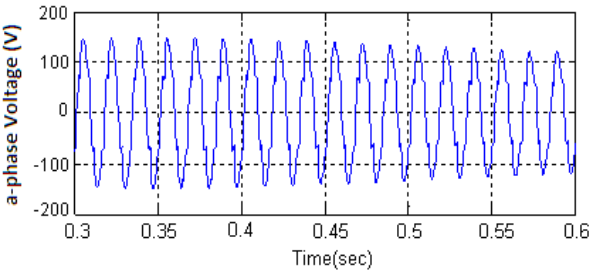

Fig. 5 A-phase voltage during transient

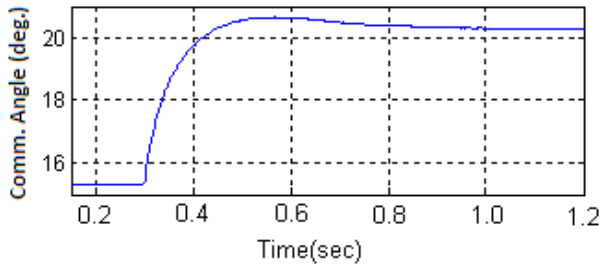

Fig. 6 Variation of commutation angle

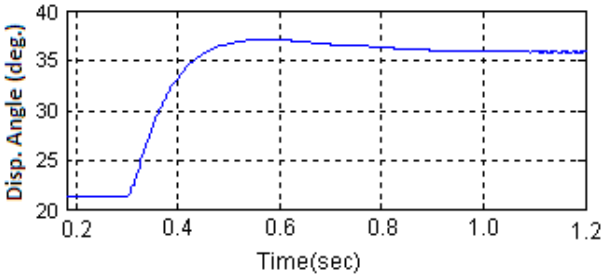

Fig. 7 Variation of displacement angle

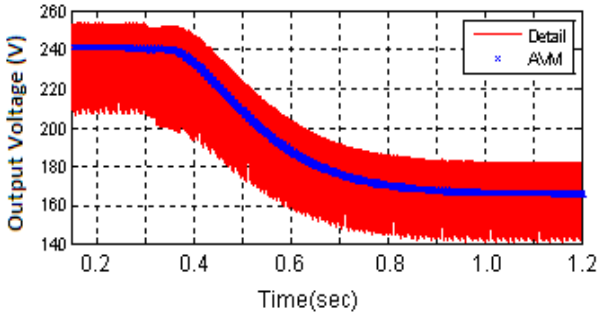

Fig. 8 Rectifier output voltage

If load resistance decreases to 2.2 Ω, the commutation will be continuous. In another study, the load resistance is decreased to 1.42 Ω at time t=0.2 sec. The load current and a-phase voltage are plotted in Figs. 9 and 10. Also, Figs. 11-13 represent the variation of commutation delay, displacement angle and output dc voltage during transient in continuous commutation mode.

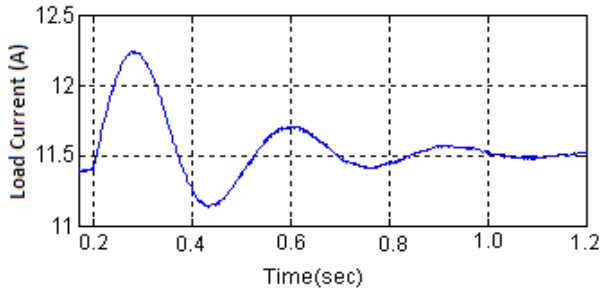

Fig. 9 Rectifier load current

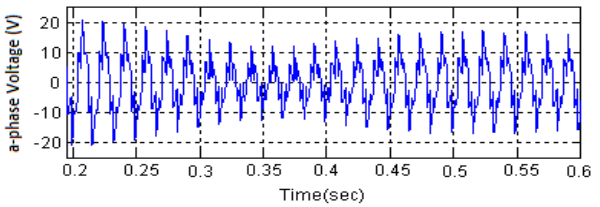

Fig. 10 A-phase voltage during transient

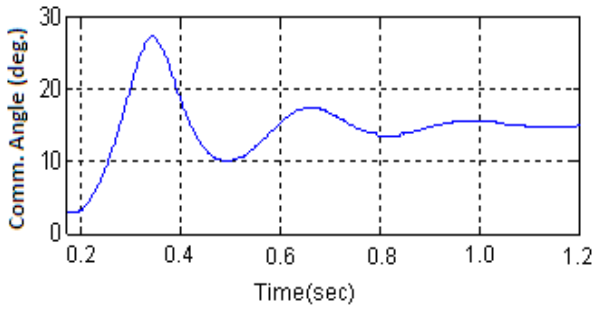

Fig. 11 Variation of commutation delay

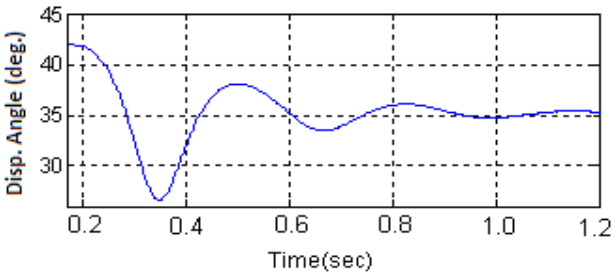

Fig. 12 Variation of displacement angle

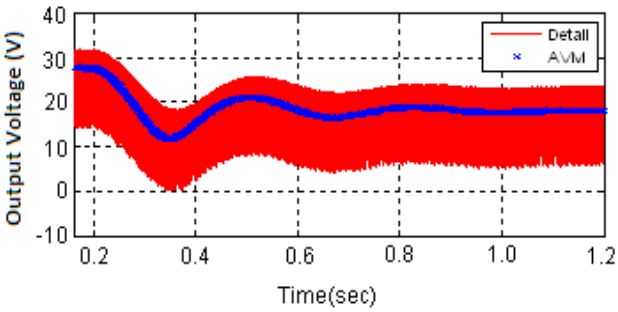

Fig. 13 Output voltage in continuous commutation mode

When load resistance changes, the load current increases rapidly and the field current rises in order to maintain constant flux. Then, with constant field voltage, the field current will decrease and the flux in the generator drops. This reduces the back emf which causes the load current to decrease.

These figures show that the average value model portrays the response of the detailed model with acceptable accuracy. Variation of load current during load step change yields the variation of commutation and displacement angles as presented in Figs. 6, 7 and

12. Because the stator transients are incorporated into the average value model of generator-converter system, even the transient of the load current is accurately captured. Also, as can be seen in Figs. 7 and 12, the displacement angle is considerable and cannot be neglected for average value modeling of rectifier operation.

5 Conclusion

The efficient voltage-behind-reactance model used for synchronous generator is suitable for determining of commutation displacement angle. Closed-form expressions are obtained to describe the system behavior. So, the circuit dynamics can be easily included in the average model. A detailed switching model was implemented and validated against experimental measurements. Finally, the described average value model was successfully evaluated against detailed simulation and its efficiency in transient conditions was demonstrated. The dc voltage obtained from the average value model is closed to the mean value of detailed simulation.

References

[1] Jadric I., Borojevic D. and Jadric M., "Modeling and control of a synchronous generator with an active DC load," *IEEE Trans. Energy Convers.*, Vol. 15, No. 2, pp. 303–311, Mar. 2000.

[2] Jatskevich J., Pekarek S. D. and Davoudi A., "Parametric average-value model of a synchronous machine rectifier system," *IEEE Trans. Energy Convers.,* Vol. 21, No. 1, pp. 9-18, Mar. 2006.

[3] Jatskevich J., Pekarek S. D. and Davoudi A., "Fast procedure for constructing an accurate dynamic average-value model of synchronous machine-rectifier systems," *IEEE Trans. Energy Convers.*, Vol. 21, No. 2, pp. 435-441, Jun. 2006.

[4] Jatskevich J., Walters E. A., Lucas C. E. and Lamm P. T., "Average-Value Model of a High-Frequency Six-Phase Generation System," *SAE Power Systems Conference*, Reno, Nevada, 2004.

[5] Jatskevich J. and Pekarek S. D., "Six-phase synchronous generator-rectifier parametric average value modeling considering operational modes," *HAIT Journal of Science and Engineering B*, Vol. 2, pp. 365-385, 2005.

[6] Krause P. C., Wasynczuk O. and Sudhoff S.D., *Analysis of Electric Machinery and drive systems*, New York: IEEE Press, chapter 11, 2002.

[7] Sudhoff S.D. and Wasynczuk O., "Analysis and average-value modeling of line-commutated converter-synchronous machine systems," *IEEE Trans. of Energy Conversion*, Vol. 8, No. 1, pp. 92-99, Mar. 1993.

[8] Sudhoff S. D., "Analysis and average-value modeling of dual line-commutated converter – 6 phase synchronous machine systems," *IEEE Trans. of Energy Conversion*, Vol. 8, No. 3, pp. 411-417, Sep. 1993.

[9] Vahedi A. and Ramezani M., "Analysis of converter-permanent magnet synchronous machine set by improved average-value modeling", *Iranian Journal of Electrical & Electronic Engineering*, Vol. 1, No. 2, pp. 81-87, April 2005.

[10] Aliprantis D. C., Sudhoff S. D. and Kuhn B. T., "A brushless exciter model incorporating multiple rectifier modes and preisach's hysteresis theory," *IEEE Trans. Energy Convers.,* Vol. 12, No. 1, pp. 136-147, Mar. 2006.

[11] Kappatou J., Safacas A., "Study of commutation phenomena and faults in a system consisting of a synchronous generator and a controlled rectifier", *European Transactions on Electrical Power*, Vol. 10, No. 1, pp. 45-52, Jan./Feb. 2000.

[12] Baghramian A. and Forsyth A. J., "Averaged-value models of twelve-pulse rectifiers for aerospace applications," *Second International Conference on Power Electronics, Machines and Drives* (PEMD2004)*,* Vol. 1, UK, 2004.

[13] Han L., Wang J. and Howe D., "State space average modelling of 6- and 12-pulse diode rectifiers," *12th European Conf. Power Electronics Appl.* (EPE), Aalborg, Denmark, 2007.

[14] Pekarek S. D. and Hegner H. J., "An efficient and accurate model for the simulation and analysis of synchronous machine/converter systems," *IEEE Trans. Energy Convers*., Vol. 13, No. 1, pp. 42-48, Mar. 1998.

Mostafa Shahnazari received his B.Sc. and M.Sc. degrees in 2000 and 2002 from Isfahan University of Technology (IUT) and Iran University of Science and Technology (IUST) both in Electrical Engineering respectively. He is currently working toward the Ph.D degree in Electrical Engineering with IUST. His research interests include modeling and identification of electrical machines, electric drives and DSP based control systems.

Abolfazl Vahedi, received his B.Sc., M.Sc. and Ph.D. in 1989, 1992 and 1996 from Ferdowsi Mashhad University, Institut Nationale Polytechnique de Lorraine (INPL-FRANCE) and INPL all in electrical engineering respectively. Currently, he is an associate professor in electrical engineering department of Iran University of Science and Technology, Tehran, Iran. He has directed several projects in the area of conventional and special electric machines and drives. His research interests are mainly design, implementation and optimization of electric machines including traction motors and drives. He is a member of Center of excellence for power system automation and operation at Iran University of Science and Technology. He is also member of IEE and SEE.